Article

Performance Evaluation of Emerging Perovskite Photovoltaic Energy-Harvesting System for BIPV Applications

Yerassyl Olzhabay [1], Muhammad N. Hamidi [2], Dahaman Ishak [2], Arjuna Marzuki [3], Annie Ng [1,4,*] and Ikechi A. Ukaegbu [1,*]

1   Department of Electrical and Computer Engineering, School of Engineering and Digital Sciences, Nazarbayev University, Astana 010000, Kazakhstan; yerassyl.olzhabay@nu.edu.kz
2   School of Electrical and Electronic Engineering, Universiti Sains Malaysia, Nibong Tebal 14300, Malaysia; najwan@usm.my (M.N.H.); dahaman@usm.my (D.I.)
3   School of Science and Technology, Wawasan Open University, George Town 10050, Malaysia; arjunam@wou.edu.my
4   National Laboratory Astana, Nazarbayev University, Astana 010000, Kazakhstan
*   Correspondence: annie.ng@nu.edu.kz (A.N.); ikechi.ukaegbu@nu.edu.kz (I.A.U.)

Abstract: Perovskite solar cells (PSCs) are emerging photovoltaics (PVs) with promising optoelectronic characteristics. PSCs can be semitransparent (ST), which is beneficial in many innovative applications, including building-integrated photovoltaics (BIPVs). While PSCs exhibit excellent performance potential, enhancements in their stability and scalable manufacturing are required before they can be widely deployed. This work evaluates the real-world effectiveness of using PSCs in BIPVs to accelerate the development progress toward practical implementation. Given the present constraints on PSC module size and efficiency, bus stop shelters are selected for investigation in this work, as they provide a suitably scaled application representing a realistic near-term test case for early-stage research and engineering. An energy-harvesting system for a bus stop shelter in Astana, Kazakhstan, demonstrates the potential performance evaluation platform that can be used for perovskite solar cell modules (PSCMs) in BIPVs. The system includes maximum power point tracking (MPPT) and charge controllers, which can supply PSCM energy to the electronic load. Based on our design, the bus stop shelter has non-transparent and ST PSCMs on the roof and sides, respectively. May (best-case) and December (worst-case) scenarios are considered. According to the results, the PSCMs-equipped bus stop shelter can generate sufficient daily energy for load even in a worst-case scenario.

Keywords: perovskite; building-integrated photovoltaics; bus stop shelter; performance; semitransparent perovskite; energy generation

1. Introduction

To suppress the rate of global warming, the continuous development of renewable energy is important. Solar energy is clean and readily available. The use of high-performance PVs can efficiently convert sunlight into electrical energy, leading to ever-increasing interest in their applications for energy generation. Nowadays, BIPV is one of the most promising PV applications in our daily life, and can utilize surrounding light for powering electronics. The PV modules are usually installed on the building or integrated with the construction materials. The placement of PVs near to electronic consumers is economically beneficial, as separated land for accommodating PVs is not required. BIPVs can be applied in various contexts, such as in smart windows [1], bus shelters [2,3], facades [4,5], and rooftops [6]. Nowadays, the majority of BIPVs are based on established PV materials, such as crystalline Si (c-Si) and polycrystalline Si (poly-Si), as well as CdTe [4,5].

Recently, a new class of photovoltaic materials, namely metal halide perovskites, have made a breakthrough in the performance of emerging PVs due to their promising intrinsic

material properties, such as high carrier mobility, a long carrier diffusion length, and a large absorption coefficient [7–9]. The record PCE of PSCs reaches 26.1% [10], which is comparable to the established PV technologies, such as c-Si (27.6% with concentrator). Moreover, PSCs can be fabricated as ST devices due to the tunable bandgaps of the light absorption materials, which cannot be achieved using conventional photovoltaics (e.g., c-Si) [8,9]. The transparency of the PSCs is also determined via the use of transparent electrodes such as indium tin oxide (ITO), fluorine-doped tin oxide (FTO), and indium zinc tin oxide (IZTO), etc. The various bandgaps of perovskite materials result in different device colors, which are suitable for the design of colored facades. Wang et al. [11] demonstrated bifacial colorful PSCs, which can harvest solar energy from both sides of the PV. This type of PV is desired for BIPV applications, where surrounding lights can enter from the front and back sides of the panels. Despite the promising properties of PSCs, the potential performance of BIPVs based on the emerging PVs has not been well-discussed. The difficulty of manufacturing large-scale PSCMs is one of the reasons. The upscaling of PSC panels reduces PCE values due to existing technical barriers, such as the nonuniformity of thin films, increased series resistance, and defect concentrations. Also, PSCs are unstable when exposed to moisture and air; thus, stability is under enhancement, and proper encapsulations are being discussed. Intensive research efforts are currently focused on addressing these challenges. Nevertheless, Panasonic Corp. announced a record PCE of 17.9% for PSCMs (>0.08 m^2) [12] in 2020. Promising advancements in large-scale PSCs have continued to be achieved in recent years, with breakthroughs being made on an ongoing basis. Meanwhile, more attention should also be placed on the system development of PSCs for BIPV applications to understand their potential for energy generation as this emerging PV technology progresses. Knowledge is needed to optimize PSC designs and integrate them into building structures to harness their full benefits and evaluate the electricity that they could provide. Energy-harvesting circuit design is vital since it contributes to the performance of the PSC. It is necessary to model the potential energy generated from BIPVs based on PSCs to accelerate the development of innovative products powered by BIPVs and realize the use of PSCs towards BIPV applications in the near future. Olatunji et al. [13] proposed a circuit for an energy-harvesting system powered by PSCs. However, this study was only focused on MPPT designs.

In this work, we propose a system design for PSCM-based BIPVs for powering the information display and LED lighting in a bus stop shelter in Astana, Kazakhstan. The bus stop shelter was chosen as an example to demonstrate the feasibility of applying current state-of-the-art PSCs in a practical setting. Compared to facades, large rooftops, and other BIPV applications, the bus stop shelter has a relatively smaller surface area and a lower demand for electronic load consumption, which is a more realistic near-term scenario that matches the current scale of PSCMs. This study utilizes the experimental data reported by prominent research groups specializing in the fabrication of large-scale PSCMs [14,15], as well as the retrieved irradiance data of Astana, the capital city of Kazakhstan, from PVsyst software, used to model PSCMs and simulate an energy-harvesting circuit for a bus stop shelter in Matlab Simulink. The electrical energy is generated from non-transparent PSCMs as well as ST PSCMs installed on the roof and three sides of the bus shelter, respectively. The excessive energy generated from the BIPVs is stored in rechargeable batteries for powering the lighting and information display, even during low illumination. In order to increase the final open-circuit voltage (V_{OC}), the solar cells are connected in series. Usually, the voltage of the conventional PV modules is 24 V, 48 V, or higher, and more research efforts are still required to optimize the design of PSCMs for higher voltages. Currently, a single-junction PSC usually has a V_{OC} from 1.0 V to 1.2 V, which is too low for BIPV applications. The series connection of individual PSCs can increase the voltage output of PSCMs. Numerous studies have successfully demonstrated the ability of a series connection of PSCs [14,15] to increase the module voltage. Higuchi and Negami [14] demonstrated the use of a PSCM with a V_{OC} of 38.6 V obtained from 35 serially connected PSCs. Rai et al. [15] fabricated a PSCM based on seven serially connected PSCs yielding a V_{OC} of 6.96 V. It should be noted

that a higher voltage output is required for BIPVs compared to the application of PVs for powering low-energy consumption devices. For example, IoT devices usually require 3.3 V to 5 V [16]. Therefore, a proper circuit should be proposed for using PSCs in the application of BIPVs. In this work, the MPPT controls the duty cycle of the boost converter to enhance the energy-harvesting potential of the PSCM. The generated electrical energy is stored in lead–acid batteries with a terminal voltage of 48 V, while the charge controller is used to ensure the proper charging of the battery. A secondary converter is required to step down the battery output voltage from 48 V to match the load voltage. LED lighting and an information display powered by a DC supply are considered in this work as they are the common energy-consuming electronics used in a bus stop shelter. The results of this work will provide engineers with important information so that they may build future effective BIPV systems based on emerging technologies. Moreover, this work is an important linkage between material engineering and electronic engineering, providing useful information for researchers in both disciplines so that they may consider the requirements for future practical PSC applications in BIPVs.

2. Methodology

2.1. Background

Kazakhstan is one of the largest landlocked countries in the world, with a land area of 2.7 million km^2. Building transmission lines and their maintenance, particularly in remote areas, are costly. The development of BIPVs could be one of the solutions to supplying power to remote areas at a low cost. Different regions of Kazakhstan have different levels of solar. The irradiation in the northern part of the country is lower than that in the southern part. In this work, Astana, the capital city of Kazakhstan, located in the north, is considered for evaluating the energy generated by PSCMs on a bus stop shelter. In this work, as one of the BIPV examples, a bus stop shelter is considered for PSCM deployment. The bus stop shelter BIPV consists of PSCMs deployed on the four sides of the shelter (including the roof) and an energy-harvesting circuitry designed to successfully harvest energy from the PSCMs. The energy-harvesting circuitry comprises the MPPT, which tracks the maximum power points of the PSCMs optimally; the charge controller, which safely charges the battery and provides energy to the load; a secondary DC-DC converter, which increases the voltage of PSCM generation or steps down the voltage suitable for DC loads; and an energy storage unit.

The simulations were conducted in Matlab Simulink as proof of concept. The irradiation data for each day of the year were retrieved from the PVsyst software (7.2 version). The average irradiance and temperature data for every month were calculated and used in the system simulation. The parameters of PSCMs were taken from the leading groups that have fabricated PSCMs on a large scale [14,15]. The irradiance data and PSCM parameters, based on PVsyst and the reported values [14,15], were then used in Matlab Simulink (R2021b version) to conduct simulations of the energy-harvesting system of the bus stop shelter to make a proof of concept for BIPV application in Astana. The proposed energy-harvesting system is an off-grid type, which is described in this section in terms of a system overview, its energy generation, energy storage, MPPT, charge controller, and applications.

The motivation for proposing an off-grid PV in this context is that Kazakhstan has a large land area with dispersed populations (19 million people in total, population density: 7 per km^2), which presents challenges for the traditional grid infrastructure regarding its ability to reach all areas in a cost-effective manner. Additionally, some remote communities remain unelectrified. An off-grid PV design could help address these issues by providing a standalone power solution. Moreover, PSCMs are still in the early stages of research and development (R&D). Technical difficulties constrain the viability of PSCMs for very-large-scale grid-tied applications. Given the current performance of PSCs, an off-grid, standalone PV system provides a more suitable application scenario aligned with the present development stage of PSCMs, and suggests a practical interim solution for the

initial evaluation of PSCM energy generation for a relatively small-scale application (i.e., bus stop shelter).

Ranjit et al. [17] developed a PV-powered system that can be implemented at an off-grid bus stop. The study was based on meteorological data. Their calculations showed that 0.608 kW could be produced daily by the system. Meanwhile, grid and off-grid bus stops were compared regarding their cost-effectiveness. The data showed an estimated payback period of 10 years for off-grid installation. Off-grid designs are commonly considered for PV application in bus stop shelters [18–20]. An off-grid BIPV utilizes the energy generated by PVs, which is autonomous, and the excess energy can be stored for later use. Building grid infrastructure is usually expensive. Thus, it is not cost-effective for countries with dispersed populations, large land areas, and electricity-scarce regions. However, using PSCMs will contribute to reducing the total cost of this standalone system and make them more cost-effective.

2.2. System Overview

The bus shelter consists of four planar sides labeled as (i) roof, (ii) Side 1 (east), (iii) Side 2 (south), and (iv) Side 3 (west) (see Figure 1). The roof provides the surface for installing non-transparent PSCMs, whereas the other sides of the bus stop shelter are equipped with ST PSCMs. The PSCMs on the roof are one of the primary energy generation units besides Side 2 (south). The PSCMs on Side 1 (east) and Side 3 (west) generate less electric energy compared to the PSCMs on Side 2 since Side 2 (south) has a larger surface area for placing PSCMs. The non-nontransparent PSCMs placed on the roof can prevent direct sunshine from reaching the people standing in the bus stop shelter, while the ST PSCMs placed on Side 1 (east), Side 2 (south), and Side 3 (west) do not block the vision of the people waiting at the bus stop. The bus stop shelter requires lighting and an information display powered by PSCMs. The excessive energy generated by the PSCMs is stored in rechargeable batteries, which can provide electric power to the loads during low illumination. In Astana, the south face has a higher illumination value than other orientations. Therefore, in this design, Side 2 faces south to collect more sunlight to generate a higher amount of electrical energy. The bus stop shelter's length L, width W, and height H are 4.5, 1.5, and 2 m, respectively. Thus, the roof's PSCM is placed in an area of L × W. Sides 1 and 3 have a surface area of W × H, and the largest ST PSCM is placed at Side 2 in an area of L × H.
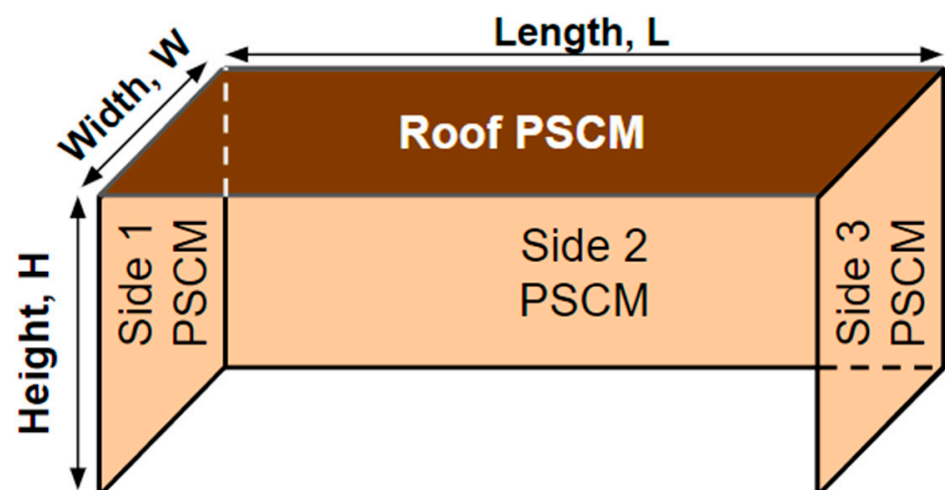

Figure 1. The design of the bus stop shelter equipped with PSCMs.

Figure 2 demonstrates the general electronic structure of the energy-harvesting system and control system for the bus shelter. The system comprises PSCMs as the energy-generating units; MPPTs with a built-in DC-DC converter for maximizing the energy-harvesting potential of the PSCMs; charge controllers for ensuring the safe charging of

batteries; and rechargeable batteries for the storage of the excess energy generated by PSCMs. The secondary converter is a DC-DC converter used to step down the voltage suitable for DC loads. The energy generated by PSCMs primarily supplies the loads (lighting and information display), whereas the excess energy generated charges the batteries. On the contrary, if the energy generated by PSCMs is insufficient to feed the loads, the batteries will complement the energy in order to power the loads. The batteries will be the only energy supply during the night for powering the loads.
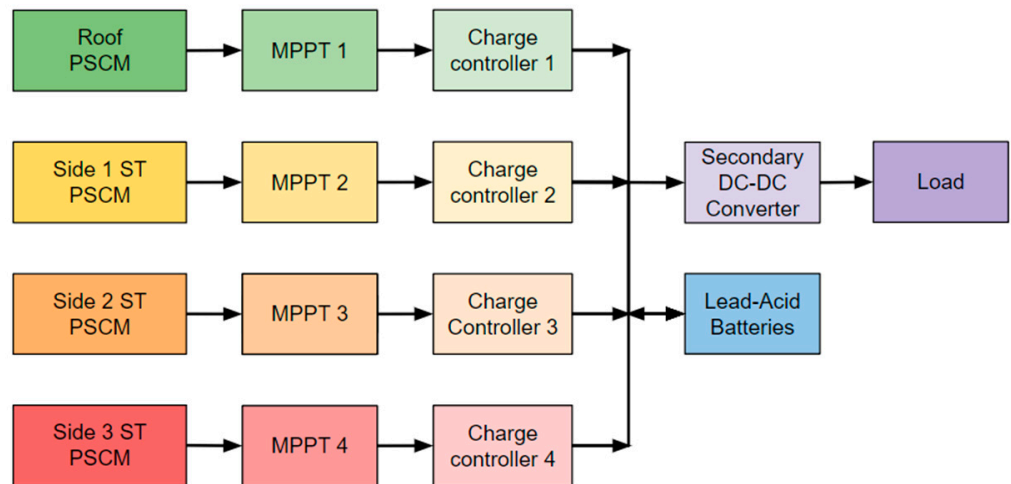

Figure 2. The proposed energy-harvesting system and control system for the bus shelter.

Figure 3 represents the proposed off-grid BIPV system type. The schematic of the proposed system circuit for the roof is illustrated in Figure 3, with Side 1 (east), Side 2 (south), Side 3 (west), and the roof having identical circuits. Each MPPT probes the PV voltage and current to run the algorithm. The charge controller probes the battery voltage and chooses the charging stage to charge the battery safely. The pulse width modulation (PWM) is produced from the charge controller to adjust the duty cycle D of the boost converter. The outputs of the converters are connected in parallel with the batteries and the load. The input V_{IN} and output voltages V_{OUT} are related, as follows [21]:
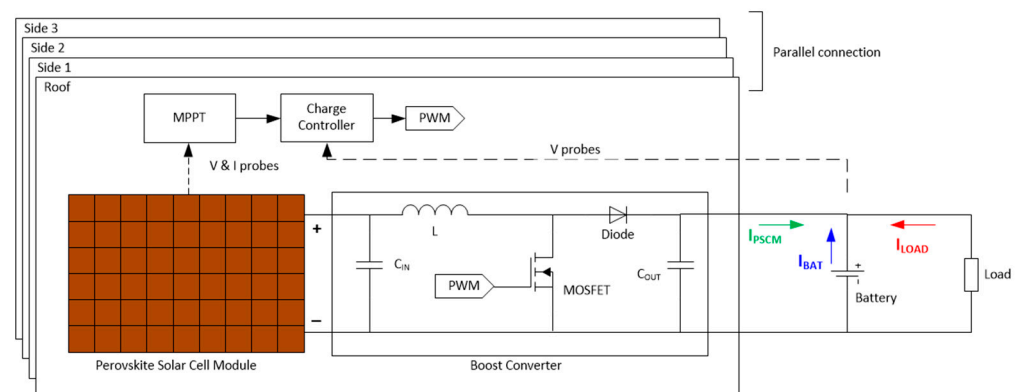
$$V_{OUT} = V_{IN}/(1 - D). \tag{1}$$

Figure 3. The schematic of the proposed energy-harvesting system and control system of the bus stop shelter.

2.3. Energy Generation

PSCMs are PV modules consisting of PSCs that are interconnected in a designed manner. To increase the output voltage of the module, PSCs are connected in series. And to increase the current generated by the PSCMs, PSCs are connected in parallel. Non-transparent PSCMs have a V_{OC} of 38.6 V, whereas ST PSCMs have a V_{OC} of 6.96 V [14,15]. Thus, 6 ST PSCMs are connected in series to obtain V_{OC} values close to those generated by non-transparent PSCMs.

The energy generated by the roof PSCMs and Side 2 (south) is more significant than that generated by the other sides of the bus stop shelter because these surfaces face irradiance-rich directions. The values of effective global irradiance at different sides of the bus shelter in Astana are summarized in Table 1, based on the data retrieved from the PVsyst. It shows the values of the monthly global effective irradiance for the PSCMs directed to the corresponding side. The PSCMs facing the north generate significantly less power; thus, the three sides of the bus stop shelter are designed to face the east, south, and west directions. Based on the data in Table 1, the roof and the south-facing side have similar total global effective irradiance values for the year. The east and west-facing sides have similar low irradiance values. Therefore, the primary energy generated by the PSCMs should come from the roof and the south-oriented side. For other cities, the difference between these two orientations will increase due to the elevation difference: the closer the city is to the south, the higher the elevation angle of the sun, etc. Therefore, most of the energy generated by PSCMs will shift to the roof rather than the south-facing side installations.

Table 1. Monthly effective global irradiance for different sides of the bus stop shelter in Astana, retrieved from PVsyst.

Monthly Global Effective Irradiance for Different Bus Shelter Sides	Roof (kWh/m^2)	Side 1 East (kWh/m^2)	Side 2 South (kWh/m^2)	Side 3 West (kWh/m^2)	Total (kWh/m^2)
January	29.1	24.2	88.5	26.2	168
February	53.1	43.1	116.1	46.0	258.3
March	104.6	77.1	139.3	77.1	398.1
April	136.4	88.2	109.6	92.4	426.6
May	191.6	123.0	108.8	121.5	544.9
June	191.6	117.2	92.2	121.3	522.3
July	178.4	112.0	91.9	110.1	492.4
August	150.6	98.2	104.4	99.1	452.3
September	101.7	69.7	103.0	70.4	344.8
October	61.7	44.2	95.0	45.7	246.6
November	30.7	23.9	66.6	24.7	145.9
December	21.6	20.7	82.9	23.2	148.4
Year	1251	842	1198	858	4149

In this work, the non-transparent PSCMs with a PCE of 12.6% measured at an aperture area of 0.0354 m^2 [14], and the ST PSCMs with a PCE of 9.5% with an active area of 0.0021 m^2 [15] were used for calculation (Figure 4). The current, voltage, and power at the maximum power point of 1000 W/m^2 are indicated in Figure 4. The PSCMs were modeled in the Matlab Simulink software to obtain similar I–V curves, as reported in the reference papers. The number of PSCMs connected in series can be altered for different cities according to the irradiance level and system performance. In this work, it is assumed that the roof, Side 1 (east), Side 2 (south), and Side 3 (west) have surface areas of 6.75, 3, 9, and 3 m^2, respectively. The roof contains 100 PSCMs, with Side 1 (east) and Side 3 (west) having 624 ST PSCMs, and Side 2 (south) having 1248 ST PSCMs. The PSCMs are connected, as demonstrated by the block diagram in Figure 2. The output terminals of the

PV are connected to the individual MPPTs, followed by the charge controller. MPPTs can maximize the energy-harvesting potential of PSCMs. A charge controller is placed after the MPPT to adjust the voltage produced by the built-in boost converter.
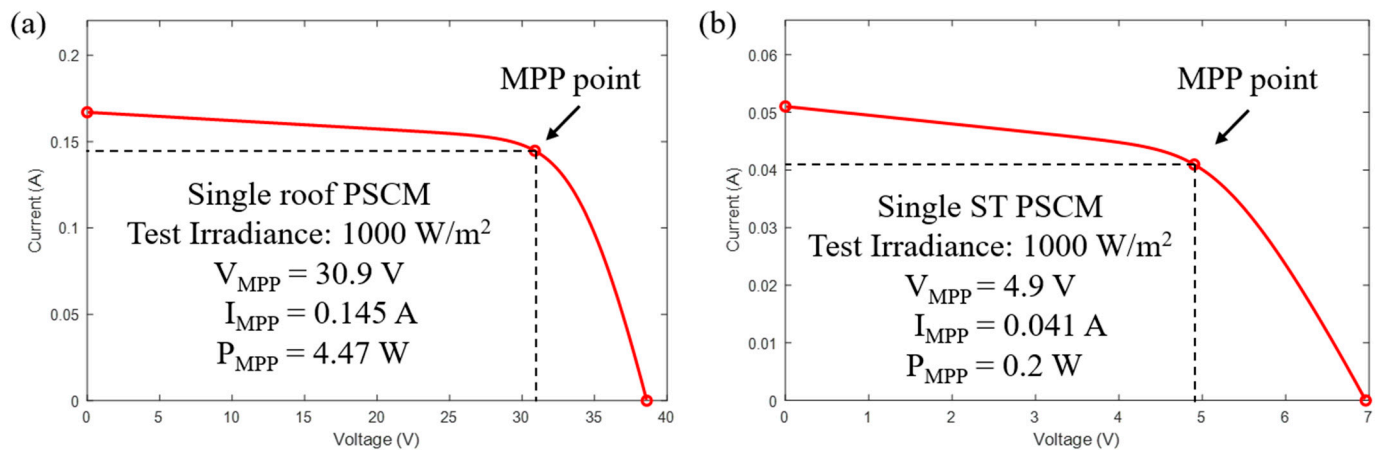
Figure 4. (**a**) I–V curve of non-transparent PSCM with an aperture area of 0.0354 m^2 used in the calculations [14]. (**b**) I–V curve of ST PSCM with an active area of 0.0021 m^2 [15]. The values in (**a**) and (**b**) indicate voltage, current, and power at the maximum power point for a single PSCM at 1000 W/m^2 irradiance.

2.4. Energy Storage

During active sun hours, the energy generated by PSCMs will be in excess. Rechargeable batteries can store the excess energy generated in order to power the loads at night. In this work, the series connection of the batteries increases the voltage, which is desired for using large PSCMs with higher generated voltages. Furthermore, using 48 V lead–acid batteries can reduce the current flow generated by the PSCMs more than lead–acid batteries with 12 V can. If the battery terminal voltage is decreased, the design of the PSC interconnection in the PSCM is required. A step-down DC-DC converter can be used if the PSCM generation produces a higher voltage than the battery terminal.

The battery capacity was determined based on the calculated load power consumption and the intended duration of autonomy. The required battery capacity was calculated by multiplying the daily load energy usage with the desired number of autonomous days. It should be noted that real-world systems are associated with some energy losses; therefore, the battery specification is made slightly larger than the calculated minimum needed. In this study, a 50 Ah battery (at 48 V) was selected. With this capacity, it was estimated that the fully charged battery could independently power the loads for a couple of days without being recharged by the PV panels.

2.5. Maximum Power Point Tracking

The MPPT is used to maximize the energy-harvesting potential of the PV. The MPPT adjusts the duty cycle of the DC-DC converter during energy generation so that the PSCM is at maximum power point. Olzhabay et al. [16] used a fractional open-circuit voltage (FOCV) MPPT algorithm to enhance the PSC energy generation capability. The FOCV approach is based on probing the V_{OC} of the PV and multiplying it by the constant to obtain an approximate maximum power point voltage value. The comparator compares this value with the probed voltage of the PV during operation. Another widely used MPPT approach is the perturb and observe (P&O) algorithm, which requires an additional current probe apart from the voltage probing. P&O further uses current and voltage probes to compare the power and voltage values of recently probed data with the saved ones. Olatunji et al. [13] proposed an MPPT circuit based on the P&O algorithm. Sample and hold circuits are added to decrease the sampling time and reduce power loss during the maximum power point. Another popular MPPT algorithm is incremental conductance,

which offers faster and more precise tracking than P&O. However, it requires a complex circuit, which adds cost to the system. Jois et al. [22] proposed a new MPPT schematic based on incremental conductance (INC) for facade BIPV. The system has many converters and grid connections. Moreover, INC requires accurate knowledge of PV parameters, which can be problematic for emerging PV technologies such as PSCs, which are in R&D.

This study uses a hill-climbing (HC) MPPT approach since the P&O method can experience oscillations when a maximum power point is achieved. The flowchart of the HC algorithm is presented in Figure 5 [23]. The voltage (V_K) and current (I_K) probes are sensed using the PSCMs. Then, after multiplying the probed voltage and current values, the power (P_K) for that moment is calculated. This power (P_K) and the probed voltage (V_K) values are compared with the previous power (P_{K-1}) and voltage (V_{K-1}) values. According to the difference between the power (P_K-P_{K-1}) and the voltages (V_K-V_{K-1}), the duty cycle (D) is changed by the duty cycle step (ΔD).
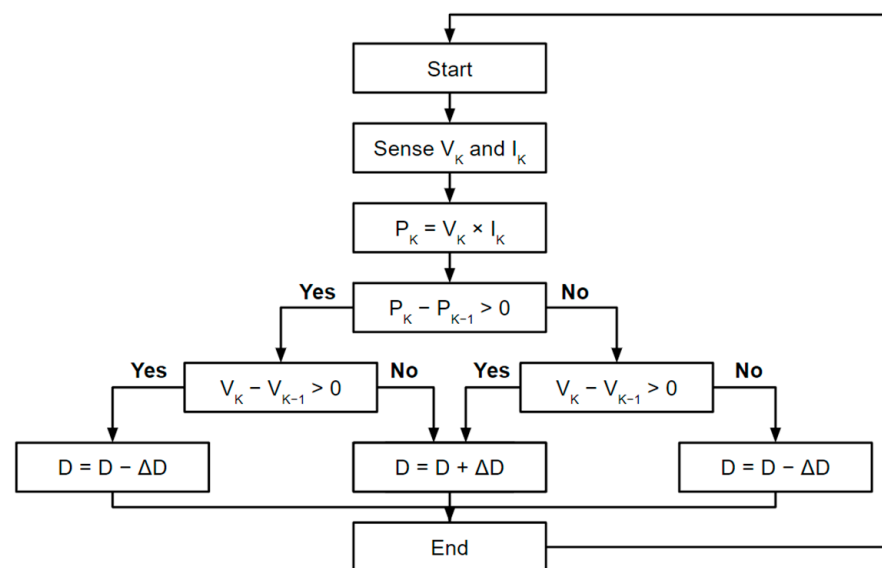
Figure 5. Flowchart of the hill-climbing MPPT algorithm.

2.6. Charge Controller

The charge controller regulates the battery-charging process to ensure safety. The charge controller probes the voltage of the battery and the duty cycle from the MPPT. Depending on the battery voltage, the charge controller produces the PWM signal to control the built-in boost converter. The charge controller has three stages [24]. During the first stage, a constant current is preserved. The second stage maintains a constant voltage when the battery is almost full. The last stage is the floating stage, when the battery is fully charged.

2.7. Applications

For the load in this work, lighting and display are used. Lighting is provided using three 3 W LEDs. The longest dark time in Astana is about 16 h in December [25]. The information display is rated as 25 W. A single-color LED display has a power consumption of less than 25 W. The information display is set to work for 24 h. The display can be turned off when the information is unavailable to reduce power consumption. Such an approach can be provided using timers or a microcontroller. Since the loads are parallel-connected with the batteries, the loads should have a DC-DC converter to decrease the battery voltage (48 V) to the desired value (5–12 V).

3. Results

In this section, the estimated energy generated by the PSCMs is calculated. Matlab Simulink was used to verify the working concept of the BIPV energy generation for Astana in December, which is the worst-case scenario for energy generation. The best-case scenario for Astana, which occurs in May (see Table 1), was also considered for comparison between these representative cases. The average temperatures in May and December are 14.3 and −11.4 °C [26], respectively. The individual roof module has the dimensions of 203 × 203 mm, with an active area of 0.0354 m² [14]. The individual ST PSCM used in the bus shelter sides has the dimensions of 6 × 6 cm, with an active device area of 0.0021 m² [15]. The 1.5 × 4.5 m roof is in a configuration in which 100 non-transparent PSCMs are connected in parallel (1s100p) to increase the generated current. The roof perovskite module has a V_{OC} of 38.6 V (13); thus, a small voltage boost is required to match the battery voltage. The ST PSCM has a V_{OC} value of 6.96 V, so six modules are connected in series to reduce the voltage difference with the battery. Side 1 (east) and Side 3 (west) have six serially connected PSCMs and 104 modules connected in parallel (6s104p) in the PSCM configuration. Side 2 (south) has twice as many parallel connections as Side 1 (east) and Side 3 (west) (i.e., 6s208p).

Table 1 shows the highest irradiation values for the four sides in May. The average hourly irradiation values are presented in Figure 6. Irradiation is present between 6:00 and 20:00. The ambient temperature increases from the morning until 15:00, then decreases. In May, the roof experiences more irradiation than Side 2 (south), which faces the south. For the northern hemisphere, the position of the sun is higher in May than in December. Therefore, Side 2 (south) experiences more irradiation than the roof in December.
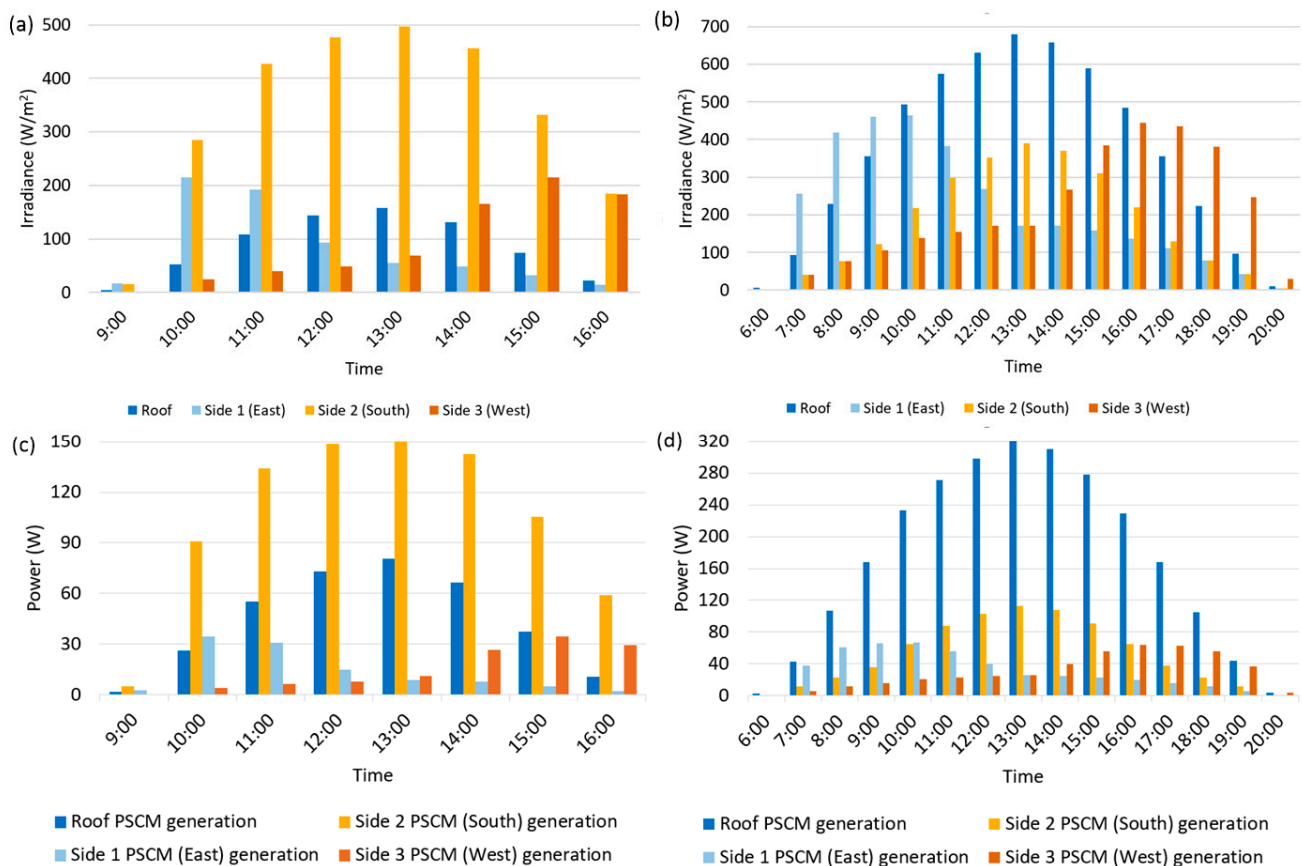
Figure 6. Global effective irradiance for bus stop shelter sides (**a**) in December and (**b**) in May, extracted from PVsyst. Energy generated by bus stop shelter during (**c**) December and (**d**) May, according to the simulation results.

The results for December are represented in Figure 6c for the bus stop shelter. The Side 2 (south) PSCMs contribute the most to energy generation. The Side 1 (east) PSCMs generate energy more efficiently during the morning, whereas the Side 3 (west) PSCMs generate energy more efficiently in the afternoon. The total daily energy generated by the roof, Side 1 (east), Side 2 (south), and Side 3 (west) PSCMs is 0.351 kWh, 0.106 kWh, 0.840 kWh, and 0.119 kWh, respectively.

The energy generated by the bus stop shelter in May is illustrated in Figure 6d. The roof PSCMs contribute the most to the total energy generation, followed by the Side 2 (south) PSCMs and then by the Side 1 (east) and Side 3 (west) PSCMs. Similar energy generation trends are observed in December for the Side 1 (east) and Side 3 (west) PSCMs. The total energy generated during the day by the roof, Side 1 (east), Side 2 (south), and Side 3 (west) PSCMs is 2.58 kWh, 0.456 kWh, 0.778 kWh, and 0.446 kWh, respectively.

The energy generated by the PSCMs on the bus stop shelter in May is several times larger than that in December. Except for the Side 2 (south) PSCMs, the energy generated by the Side 1 (east) and Side 3 (west) PSCMs is at least four times greater than that generated in December. The PSCM on the roof generates almost seven times more power in May than in December. The load in this work consumed 0.744 kWh daily. The energy generated by the bus stop shelter in December is still sufficient to supply the load and store excess energy in the batteries.

Figure 7 demonstrates the waveforms for the roof PSCM with MPPT operation for the resistive load. Figure 7a includes the I-V curve of the roof PSCM at 25 °C. The current I_{MPP}, voltage V_{MPP}, and power P_{MPP} at the maximum power point are 9.87 A, 31.2 V, and 308 W, respectively (refer to Figure 7). Figure 7b illustrates how the input (red) and output (green) currents vary as the maximum power point is achieved. It can be seen that, as the input current increases, so does the output current. The values of the input and output currents are 9.84 A and 5.53 A, respectively, when settled. The blue line in Figure 7b is the current when the roof PSCM is at the maximum power point. Figure 7c,d show the voltage and power waveforms during MPPT operation. The MPPT sets the converter so that the PSCM is able to generate the maximum power. By doing so, the input voltage reaches V_{MPP}. The input and output power get to the power at the maximum power point. The input power is higher than the output power due to power loss during the conversion. At the end of the waveforms, the input and output voltages are 31.3 V and 55.26 V, respectively. The input and output powers are 308 W and 305 W, respectively. The mean efficiency of the MPPT is kept at around 98%.

3.1. Case Studies

This section presents the difference between the morning and afternoon time in May and December, the best-case and the worst-case energy generation. The average data are considered during calculation.

3.1.1. May 9:00

Figure 8a illustrates the total current coming from the PSCM (green), battery (blue), and load (red) currents. Before the maximum power point is achieved, the battery complements PSCM generation to feed the load until the PV generation is sufficient. As PSCM generation is enough to supply the load, excess energy charges the battery. There are current waveform fluctuations due to MOSFET switching on and off in the boost converters. Moreover, the fluctuation peaks also increase since there are four sides of the bus stop shelter. The battery voltage is 47.9 V. The load is constantly at 25 W, which results in a constant current and the power curves shown in Figure 8. The value of the load current is around 0.52 A.

The power waveform graph is presented in Figure 8b. The battery helps the PSCM to feed the load at the beginning of the simulation. The battery power waveform (blue) crosses the zero of the y-axis when the PSCM can feed the load. The excess energy charges the battery, which is observed by the increasing magnitude of the current.
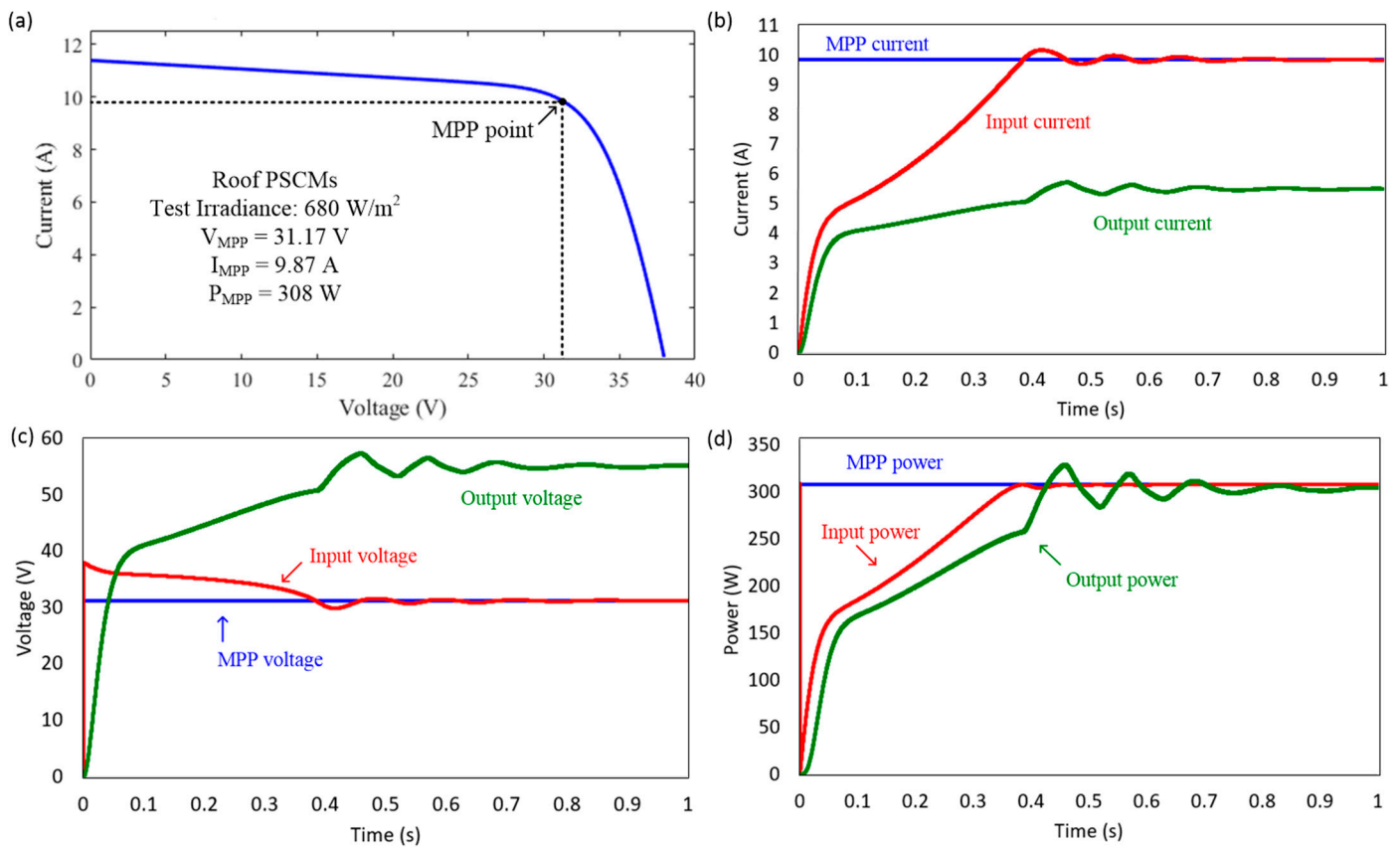
Figure 7. (**a**) I–V curve of the roof PSCMs. Input, output, and maximum power point (**b**) current, (**c**) voltage, and (**d**) power waveforms during MPPT operation on May at 13:00. The values in (**a**) represent the irradiance value and maximum power point parameters, such as the voltage, current, and power of the roof PSCM.
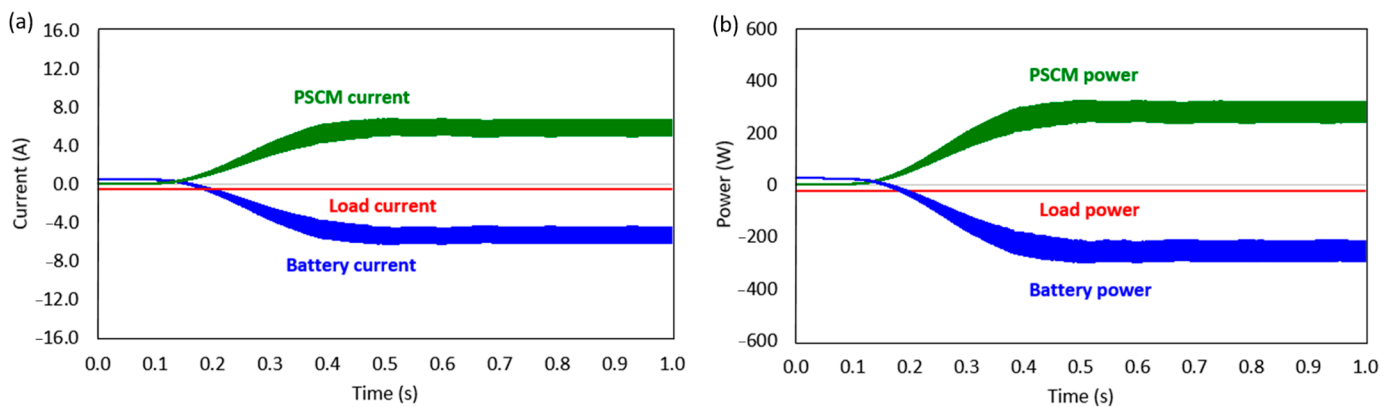
Figure 8. (**a**) Current and (**b**) power waveforms for energy-harvesting system generation, battery, and load for the May at 9:00 scenario.

3.1.2. May 13:00

At 13:00, the power generation is among the highest during the day for the given bus stop shelter. Figure 9a represents the current waveforms for this case study. The battery discharges and complements the PSCM generation, similar to the case of May at 9:00. The PSCM generation is sufficient to supply the load in a shorter time than in the previous case due to higher irradiance. This leads to higher PSCM power generation. The battery voltage is 48.0 V. The power waveforms are presented in Figure 9b. The maximum power point is achieved at a similar time as in May at 9:00.

3.1.3. December 9:00

Figure 10a represents current waveforms for the case of December at 9:00. The PSCMs of Side 1 (east) and Side 3 (west) can generate a small amount of power and require much more time to achieve the maximum power point compared to the roof and Side 2 (south) PSCMs. The roof and Side 2 (south) PCMSs contribute the most amount of power (refer to Figure 6c). The battery voltage is 47.7 V. The battery helps the PSCM generation to feed the load, as shown in Figure 10b for the entire period. Electric generation in the morning cannot feed the load without the battery.
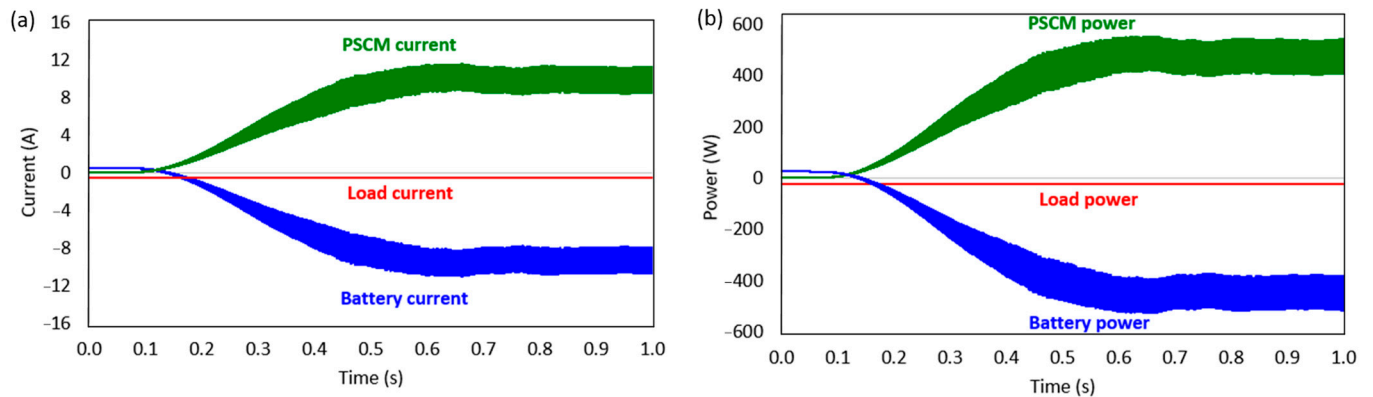

Figure 9. (**a**) Current and (**b**) power waveforms for energy-harvesting system generation, battery, and load for the May at 13:00 scenario.

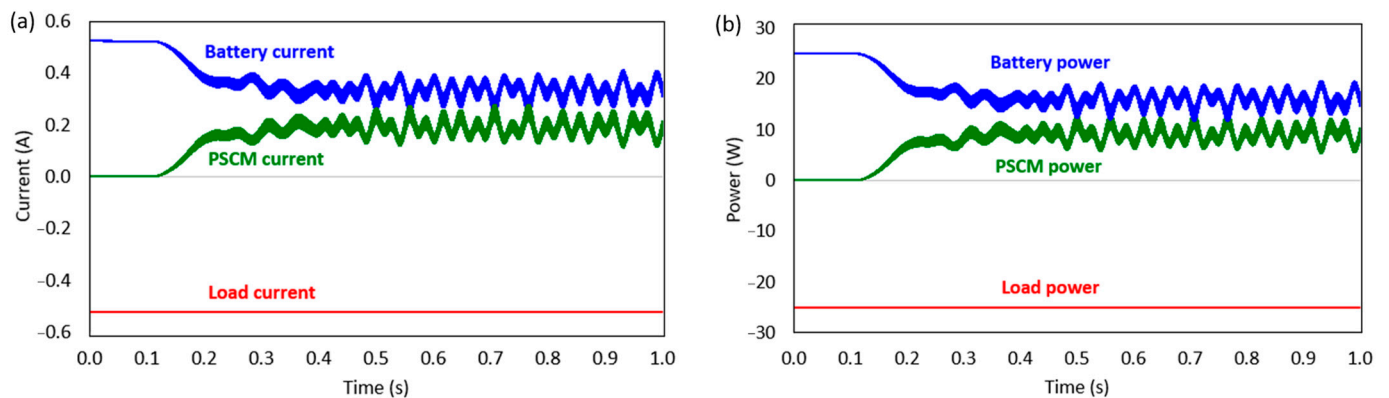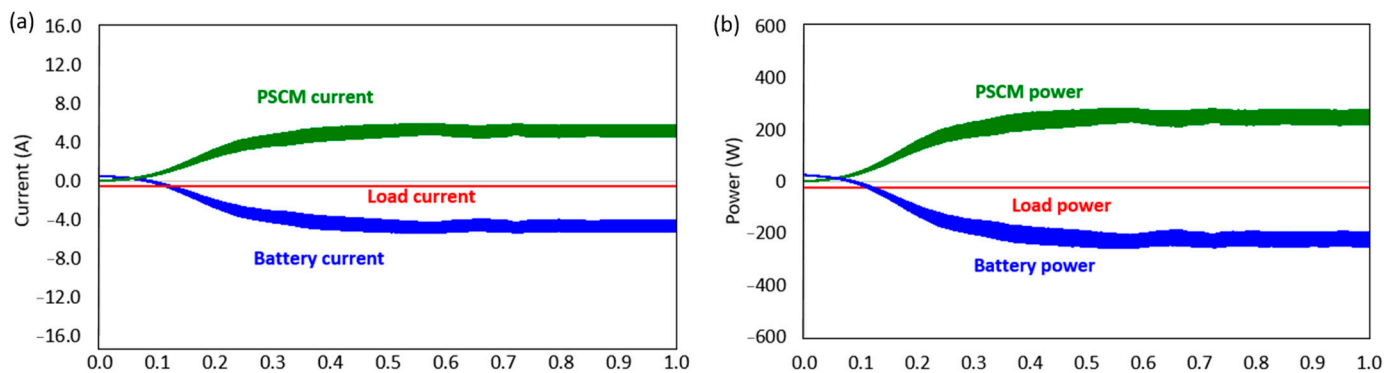**Figure 10.** (**a**) Current and (**b**) power waveforms for energy-harvesting system generation, battery, and load for the December at 9:00 scenario.

3.1.4. December 13:00

At 13:00 in December, the power generation is much higher than in the morning of December. Figure 11a illustrates the current waveforms. The PSCM power generation is sufficient to power the load. When the blue lines (battery) cross the x-axis, the excess energy generated by the PSCMs starts to charge the battery. The battery voltage is 47.9 V. According to Figure 11b, the generated power is sufficient to feed the load and charge the battery.

Figure 11. (**a**) Current and (**b**) power waveforms for energy-harvesting system generation, battery, and load for the December at 13:00 scenario.

4. Discussion

According to Table 1, from April to August, the global irradiance for the roof PSCMs is higher than that of the south-oriented PSCMs. For the rest of the year, the south-facing PSCMs receive more irradiance than the PSCMs on the roof. Hence, it is suggested that as many PSCMs as possible are placed facing the south rather than on other sides. Although the south-facing PSCMs receive relatively less irradiance during April to August (mid-spring to late summer period) when compared to other orientations, the energy generated should be sufficient since the sun hours in the summer are more than those in the winter. It should be noted that the orientation of bus stops also depends on the design of the roads. When Side 2 of the bus stop shelter faces different directions, the energy generated by the PSCMs varies accordingly, and the results are summarized in Table 2.

Table 2. PSCM energy generation in the bus stop shelter for different orientations and tilt angles.

Roof PSCM Tilt Angle	North-Oriented (kWh)	East-Oriented (kWh)	South-Oriented (kWh)	West-Oriented (kWh)
No tilt angle	19.4	25.7	32.6	25.5
32-degree	30.8	37.1	44.0	36.9

In addition, the roof part can be tilted for a better angle to maximize the light-harvesting capability of the PSCM. According to Jacobson and Jadhav [27], the optimal tilt angle for Kazakhstan is 32 degrees. In December, tilted PSCMs on the roof of bus stop shelters will receive irradiation of around 2.15 kWh/m^2 daily. Non-tilted PSCMs on the roof have an average daily irradiation of 0.695 kWh/m^2, which is three times lower than the tilted one. Table 2 summarizes the total energy generated by PSCMs with different tilt angles. The 32-degree tilting of the PSCMs results in an increase of 11.4 kWh energy generation, which is an approximately 59%, 44%, 35%, and 45% enhancement for north-, east-, south-, and west-oriented bus stop shelters, respectively.

It should be noted that this work was performed using the average daily temperature, whereas the temperature constantly changes in actual cases. The temperature affects the panel performance and alters the V_{OC} of the solar modules. The temperature can change every hour, but this uncertainty has not been considered for calculation. Moreover, the overestimation of the energy generated by PSCMs is possible due to the reflections of incoming light at the surface of the bus stop shelter. The development of anti-reflection coatings and the incorporation of nanostructures at the surface of PSCMs can minimize the reflection loss. It is possible that obstacles will block the incoming light from reaching PSCMs. In this work, shading and soiling loss are not considered. Meanwhile, it is assumed that ideal MOSFETs and diodes are used in the converters, as well as that there is no power loss for the connection wires used in the system. Notably, PSCMs have stability issues

due to the exposure of the perovskite material to moisture and oxygen. Nevertheless, intensive research efforts have been devoted to this emerging technology, resulting in continuous enhancements in PCE and the lifetime of PSCMs. Encapsulation methods are being developed to protect perovskite materials from ambient conditions and provide good sealing for lead components in the active layer.

It is worth comparing the results of this work with the existing data. Table 3 summarizes the information on some small-scale BIPV systems. Fijałkowska et al. [19] used a calculation-based method to assess the effectiveness of PV installations on bus stop shelters based on irradiation data, considering the effects of shading caused by the surrounding buildings. This off-grid bus stop shelter is in Warsaw, Poland, at an altitude of 100 m. Based on their calculations, the bus stop shelter near Rondo ONZ has the potential to generate 6.8 kWh in June and 0.3 kWh in December. For another bus stop shelter near Dworec Centralny, the values are 6.4 kWh and 0.4 kWh for June and December, respectively. The order of energy generation is close to our results obtained in this study (4.26 kWh in May and 1.42 kWh daily in December).

Table 3. Comparison of BIPV systems with the proposed PSCM-powered BIPV.

BIPV Study Parameters	[19]	[20]	[28]	This Work
Location	Warsaw, Poland;	Turin, Italy;	Zaragoza, Spain;	Astana, Kazakhstan;
Altitude (m)	100	239	243	347
System type of the study	Calculation	Experimental	Calculation	Simulation
BIPV application	Off-grid bus stop shelter	Off-grid bus stop shelter	Off-grid bus stop shelter	Off-grid bus stop shelter
PV technology	Not available	Mono-crystalline silicon	Crystalline silicon	Perovskite
PV efficiency (%)	Not available	18.6	Not specified	12.6 (roof); 9.50 (ST)
PV area (m^2)	Not available	0.89	6.00	3.54 (roof); 5.24 (ST)
System components	Not available	PV modules, Inverter (for AC load) Charge controllers, Batteries	PV modules, Batteries	PV modules, Boost converter, MPPT, Charge controller, Batteries,
Load	Not specified	Wi-Fi station, USB chargers, Air quality control	Lighting, Information screen	Lighting, Information display
Generated energy (kWh/daily)	0.30–6.80; 0.40–6.40	Not specified	2.66	1.42–4.26

Mutani et al. [20] developed a prototype of a bus stop shelter in Turin, Italy (239 m altitude). The prototype consisted of PV modules, batteries, an inverter, and charge controllers. The c-Si PV panels had an efficiency of 18.6%. An air quality sensor, Wi-Fi emitter, and USB chargers were considered as loads. However, the generated energy was not specified in the study to be compared with our work.

A PV-powered bus stop station in Zaragoza (Spain, altitude of 243 m) is one of the BIPV-built examples. The generated energy is used for the purposes of lighting and powering an information screen. The PV is based on c-Si modules with an area of 6 m^2 and a projected power generation of 34,018 kWh for 35 years (i.e., around 972 kWh annually; ~2.66 kWh daily) [28]. In comparison, the projected daily energy generation is 2.66 kWh, versus 1.42 kWh (worst-case) to 4.26 kWh (best-case) in this study. The differences between the two systems are the PV technology (crystalline silicon versus developing PSCMs) and irradiance. Zaragoza (41°39′ N 0°53′ W) is located in Spain, whereas our work considers Kazakhstan (51°08′ N 71°25′ E), which has a lower irradiance level compared to Spain. It is noted that the assumptions for the 35-year forecast of energy generation are not disclosed in the source. The performance of BIPV systems can vary substantially depending on factors like the local solar irradiance levels, the specific PV technology employed, and the geometric design characteristics inherent to different building applications. Therefore, direct comparisons of estimated energy generation among dissimilar cases must be made cautiously, as disparities in the key input parameters of different scenarios are difficult to compare precisely, particularly when the background information and reported data are not provided in detail. Transparency in the modeling assumptions would help to validate the projected performance and enable more robust cross-comparisons of different BIPV implementations over long timeframes.

5. Conclusions

Our evaluation of PSCMs integrated into bus stop shelters in Astana, Kazakhstan (51°08′ N 71°25′ E), demonstrates their potential for generating significant amounts of energy, with the bus stop shelter equipped with PSCMs generating an average daily energy output of 1.42 kWh for the worst-case scenario in December and 4.26 kWh for the best-case scenario. We observed that the daily energy generation is sufficient to power the lighting and information display throughout the day, with surplus energy stored in rechargeable batteries for use during low-illumination periods. Moreover, additional DC loads can still be adopted for the surplus energy generated in the worst-case scenario. This sustainable and cost-effective solution could be a key component of future smart city infrastructure, promoting energy efficiency, reducing reliance on the grid, and contributing to a more sustainable urban environment. With the rapid development of new-generation PSCMs, these emerging PVs will play a major role in the future of cost-effective BIPVs, paving the way for more sustainable and energy-efficient cities.

References

1. Ravula, H.; Bollapragada, S. Solar Window as an Energy Source: A Patent Study. In Proceedings of the 2020 IEEE International Power and Renewable Energy Conference (IPRECON 2020), Karunagappally, India, 30 October–1 November 2020. [CrossRef]
2. Santos, T.; Lobato, K.; Rocha, J.; Tenedório, J.A. Modeling photovoltaic potential for bus shelters on a city-scale: A case study in Lisbon. *Appl. Sci.* **2020**, *10*, 4801. [CrossRef]
3. Sánchez-Aparicio, M.; Lagüela, S.; Martín-Jiménez, J.; Del Pozo, S.; González-González, E.; Andrés-Anaya, P. Smart Mobility in Cities: GIS Analysis of Solar PV Potential for Lighting in Bus Shelters in the City of Ávila. In Proceedings of the Ibero-American Congress of Smart Cities (ICSC-CITIES 2020), San José, Costa Rica, 9–11 November 2020. [CrossRef]
4. Alrashidi, H.; Issa, W.; Sellami, N.; Sundaram, V.; Mallick, T. Thermal performance evaluation and energy saving potential of semitransparent CdTe in Façade BIPV. *Sol. Energy* **2022**, *232*, 84–91. [CrossRef]
5. Martín-Chivelet, N.; Polo, J.; Sanz-Saiz, C.; Núñez Benítez, L.T.; Alonso-Abella, M.; Cuenca, J. Assessment of PV Module Temperature Models for Building-Integrated Photovoltaics (BIPV). *Sustainability* **2022**, *14*, 1500. [CrossRef]
6. Singh, A.K.; Prasath Kumar, V.R.; Krishnaraj, L. Emerging technology trends in the C & I rooftop solar market in India: Case study on datacentre—Retrofit with BIPV by U-Solar. *Sol. Energy* **2022**, *238*, 203–215. [CrossRef]
7. Batmunkh, M.; Zhong, Y.L.; Zhao, H. Recent Advances in Perovskite-Based Building-Integrated Photovoltaics. *Adv. Mater.* **2020**, *32*, 2000631. [CrossRef] [PubMed]
8. Roy, A.; Ghosh, A.; Bhandari, S.; Sundaram, S.; Mallick, T.K. Perovskite Solar Cells for BIPV Application: A Review. *Buildings* **2020**, *10*, 129. [CrossRef]
9. Zhu, Y.; Shu, L.; Fan, Z. Recent Progress on Semitransparent Perovskite Solar Cell for Building-integrated Photovoltaics. *Chem. Res. Chin. Univ.* **2020**, *36*, 366–376. [CrossRef]
10. Best Research-Cell Efficiencies. 2023. Available online: https://www.nrel.gov/pv/assets/pdfs/best-research-cell-efficiencies.pdf (accessed on 7 September 2023).
11. Wang, H.; Dewi, H.A.; Koh, T.M.; Bruno, A.; Mhaisalkar, S.; Mathews, N. Bifacial, Color-Tunable Semitransparent Perovskite Solar Cells for Building-Integrated Photovoltaics. *ACS Appl. Mater. Interfaces* **2020**, *12*, 484–493. [CrossRef] [PubMed]
12. Champion Photovoltaic Module Efficiency Chart. 2022. Available online: https://www.nrel.gov/pv/module-efficiency.html (accessed on 10 November 2022).
13. Olatunji, S.I.; Marzuki, A.; Ng, A.; Ukaegbu, I.A. Perovskite PV MPPT Design for BIPV Application. In Proceedings of the 2023 IEEE 3rd International Conference in Power Engineering Applications (ICPEA 2023), Putrajaya, Malaysia, 6–7 March 2023. [CrossRef]
14. Higuchi, H.; Negami, T. Largest highly efficient 203 $\times$ 203 mm^2 CH3NH3PbI3 perovskite solar modules. *Jpn. J. Appl. Phys.* **2018**, *57*, 08RE11. [CrossRef]
15. Rai, M.; Yuan, Z.; Sadhu, A.; Leow, S.W.; Etgar, L.; Magdassi, S.; Wong, L.H. Multimodal Approach towards Large Area Fully Semitransparent Perovskite Solar Module. *Adv. Energy Mater.* **2021**, *11*, 2102276. [CrossRef]
16. Olzhabay, Y.; Ng, A.; Ukaegbu, I.A. Perovskite PV Energy Harvesting System for Uninterrupted IoT Device Applications. *Energies* **2021**, *14*, 7946. [CrossRef]
17. Ranjit, S.S.S.; Tan, S.F.; Subramaniam, S.K. Implementation Off-Grid Solar Powered Technology to Electrify Existing Bus Stop. In Proceedings of the 2011 Second International Conference on Intelligent Systems, Modelling and Simulation, Phnom Penh, Cambodia, 25–27 January 2011. [CrossRef]
18. Khamisani, A.A. *Design Methodology of Off-Grid PV Solar Powered System (A Case Study of Solar Powered Bus Shelter)*; Project Report; Eastern Illinois University: Charleston, SC, USA, 2019.
19. Fijałkowska, A.; Waksmundzka, K.; Chmiel, J. Assessment of the Effectiveness of Photovoltaic Panels at Public Transport Stops: 3D Spatial Analysis as a Tool to Strengthen Decision Making. *Energies* **2022**, *15*, 1230. [CrossRef]
20. Mutani, G.; Vodano, A.; Pastorelli, M. Photovoltaic solar systems for smart bus shelters in the urban environment of Turin (Italy). In Proceedings of the 2017 IEEE International Telecommunications Energy Conference (INTELEC), Broadbeach, Australia, 22–26 October 2017. [CrossRef]
21. Keeping, S. The Difference between Switching Regulator Continuous and Discontinuous Modes and Why It's Important. 2014. Available online: https://www.digikey.com/en/articles/the-difference-between-switching-regulator-continuous-and-discontinuous-modes-and-why-its-important (accessed on 13 August 2023).
22. Jois, S.; Bhosale, R.; Ramamritham, K.; Agarwal, V. Novel Scheme for Extracting Maximum Power from Façade Based Building Integrated Photovoltaics. In Proceedings of the 2019 IEEE 46th Photovoltaic Specialists Conference (PVSC), Chicago, IL, USA, 16–21 June 2019. [CrossRef]
23. Ebrahim, M.A.; Mohamed, R.G. Comparative Study and Simulation of Different Maximum Power Point Tracking (MPPT) Techniques Using Fractional Control and Grey Wolf Optimizer for Grid Connected PV System with Battery. In *Electric Power Conversion*; Găiceanu, M., Ed.; IntechOpen: Rijeka, Croatia, 2019. [CrossRef]
24. Tan, R.H.G.; Er, C.K.; Solanki, S.G. Modeling of Photovoltaic MPPT Lead Acid Battery Charge Controller for Standalone System Applications. *E3S Web Conf.* **2020**, *182*, 03005. [CrossRef]
25. Sunrise and Sunset Times in Nursultan. Available online: https://www.timeanddate.com/sun/kazakstan/astana?month=12 (accessed on 25 January 2022).

26. Astana Climate (Kazakhstan). Available online: https://en.climate-data.org/asia/kazakhstan/astana/astana-491/ (accessed on 4 October 2022).
27. Jacobson, M.Z.; Jadhav, V. World estimates of PV optimal tilt angles and ratios of sunlight incident upon tilted and tracked PV panels relative to horizontal panels. *Sol. Energy* **2018**, *169*, 55–66. [CrossRef]
28. Photovoltaic Bus Stop in Zaragoza. Available online: https://onyxsolar.com/photovoltaic-bus-stop (accessed on 20 August 2023).